AD-A052 541 AERONAUTICAL RESEARCH INST OF SWEDEN STOCKHOLM AEROD--ETC F/G 20/4
INVESTIGATION OF THE BOUNDARY CONDITION AT A WIND TUNNEL TEST S--ETC(U)
FEB 78 S G HEDMAN, H SORENSEN, S NYBERG AFOSR-77-3282

UNCLASSIFIED FAA-AU-1432 AFOSR-TR-78-0605 NL

| OF |
AD
A052541

END
DATE
FILMED
5-78
DDC

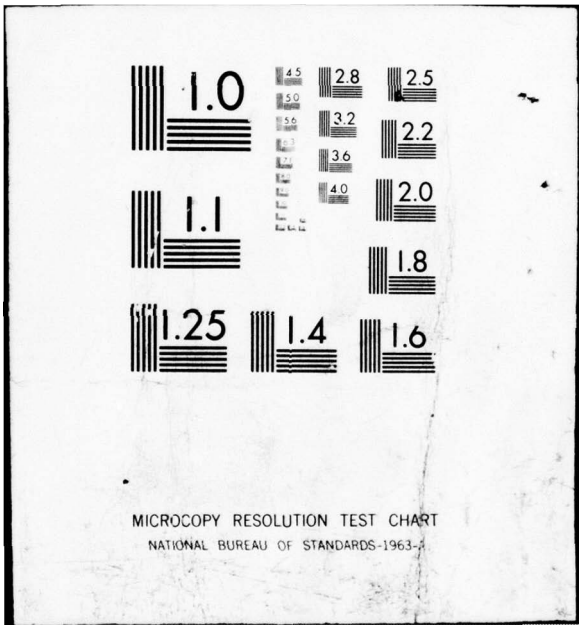
1.0
1.1
1.25
1.4
1.6
1.8
2.0
2.2
2.5
2.8
3.2
3.6
4.0
4.5
5.0
5.6
MICROCOPY RESOLUTION TEST CHART
NATIONAL BUREAU OF STANDARDS-1963-A

Grant No. AFOSR-77-3282

INVESTIGATION OF THE BOUNDARY CONDITION AT A WIND TUNNEL TEST SECTION WALL FOR A LIFTING WING BODY MODEL AT LOW SUPERSONIC SPEED

Phase 1. Test preparations, revision of computer program and exploratory computations

Sven G. Hedman, Hans Sörensén and Sven-Erik Nyberg

The Aeronautical Research Institute of Sweden (FFA)
Stockholm, Sweden

24 February 1978

[redacted] Scientific Report, 77 April 01 – 78 march [redacted] 31

Prepared for

AIR FORCE OFFICE OF SCIENTIFIC RESEARCH (AFSC)
Bolling AFB, USA

and

EUROPEAN OFFICE OF AEROSPACE RESEARCH AND DEVELOPMENT (EOARD)
London, England

by

THE AERONAUTICAL RESEARCH INSTITUTE OF SWEDEN (FFA)

This research has been sponsored in part by the AFSC and, to matched amount, by FFA

[redacted] [redacted]

SECURITY CLASSIFICATION OF THIS PAGE *(When Data Entered)*

REPORT DOCUMENTATION PAGE

READ INSTRUCTIONS BEFORE COMPLETING FORM

1. REPORT NUMBER: AFOSR-TR-78-0605
2. GOVT ACCESSION NO.
3. RECIPIENT'S CATALOG NUMBER

4. TITLE (and Subtitle): Investigation of the Boundary Condition at a Wind Tunnel Test Section Wall for a Lifting Wing Body Model at Low Supersonic Speed. Phase 1. Test preparations, revision of computer program and exploratory computations.

5. TYPE OF REPORT & PERIOD COVERED: INTERIM Rept. 1 Apr 77 - 31 Mar 78

6. PERFORMING O.R.G. REPORT NUMBER: FFA-AU-1432

7. AUTHOR(s): SVEN G. HEDMAN, HANS SÖRENSÉN, SVEN-ERIK NYBERG

8. CONTRACT OR GRANT NUMBER(s): AFOSR-77-3282 new

9. PERFORMING ORGANIZATION NAME AND ADDRESS: AERONAUTICAL RESEARCH INSTITUTE OF SWEDEN, AERODYNAMICS DEPARTMENT (FFA), PO BOX 11021, S161 11 BROMMA, SWEDEN

10. PROGRAM ELEMENT, PROJECT, TASK AREA & WORK UNIT NUMBERS: 2307A1; 61102F

11. CONTROLLING OFFICE NAME AND ADDRESS: AIR FORCE OFFICE OF SCIENTIFIC RESEARCH/NA, BLDG 410, BOLLING AIR FORCE BASE, D C 20332

12. REPORT DATE: Feb 78 (24 Feb 78)

13. NUMBER OF PAGES: 31 (34 Pl)

14. MONITORING AGENCY NAME & ADDRESS *(if different from Controlling Office)*: FFA-AU-1432

15. SECURITY CLASS. *(of this report)*: UNCLASSIFIED

15a. DECLASSIFICATION/DOWNGRADING SCHEDULE

16. DISTRIBUTION STATEMENT *(of this Report)*

Approved for public release; distribution unlimited.

17. DISTRIBUTION STATEMENT *(of the abstract entered in Block 20, if different from Report)*

18. SUPPLEMENTARY NOTES

19. KEY WORDS *(Continue on reverse side if necessary and identify by block number)*

TRANSONIC WIND TUNNELS
WALL BOUNDARY CONDITION
LOW SUPERSONIC SPEED

20. ABSTRACT *(Continue on reverse side if necessary and identify by block number)*

The purpose of this investigation is to study experimentally and theoretically the flow field at locations around a lifting wing-body model, where wind-tunnel walls are normally situated. During Phase 1, which this report covers, the preparations for the experimental investigation have been carried out. The delta-wing-body model, the sting and support arrangement, a balance and a miniature flow inclination probe have been designed and manufactured. For the theoretical calculations a relaxation method based on the transonic small perturbation equation has been used. The computer program has been revised for supersonic free stream Mach numbers. The pressure and flow deflection angle have

DD FORM 1 JAN 73 1473 EDITION OF 1 NOV 65 IS OBSOLETE

UNCLASSIFIED

SECURITY CLASSIFICATION OF THIS PAGE *(When Data Entered)*

407 117

been calculated in the field near the wing-body configuration at Mach number 1.2 and at incidences of 0° and 5°.

LIST OF CONTENTS

SYMBOLS

c	wing chord
C_p	pressure coefficient
f	function describing model surface
M_∞	free stream Mach number
U_∞	free stream velocity
x,y,z	Cartesian coordinates (mm), x in flow direction, y in spanwise direction, z upwards
α	angle of attack
δ	wing thickness ratio
ϵ	scaling factor
ϕ	velocity potential
φ	perturbation velocity potential
θ	flow deflection angle, positive out from tunnel centerline

1. INTRODUCTION

The model in a supersonic wind tunnel produces compression and expansion waves which are reflected at the test section wall. The type and the strength of the reflection depends on the wave attenuation properties of the wall. Below a certain Mach number, depending primarily on the model length in relation to its distance from the nearest test section wall, the reflected waves will hit the model and distort the pressure distribution over it.

There is today no method available to make reliable corrections for this kind of wall interference. Consequently the main research efforts during the last decades have been directed to minimizing the wall interference to such an extent that uncorrected data obtained in tunnels with wave-attenuating walls can be accepted.

Criteria for the desired cross-flow characteristics of a wave-attenuating ventilated wall have been obtained by theoretical calculations of the undisturbed flow field at a distance from the model corresponding to the position of a hypothetical wall [1] and [2]. Accurate calculation of the flow field at low supersonic free stream Mach numbers has only been possible for two-dimensional wings and for zero-lift axisymmetric bodies.

Calculations performed have shown that the required relationship between pressure drop and cross-flow for the wall varies within the flow field for the same model and also with model configuration and Mach number. It seems consequently not possible to find a fixed geometry wall that is interference-free. Some wall configurations have, however, been developed which offer an acceptable compromise between the known design requirements.

The most successful configuration, currently in use in a number of operating wind tunnels, is the differential resistance perforated wall, developed at AEDC. The differential resistance to inflow and outflow is tailored to calculated and experimentally verified requirements for cone-cylinder models and slender continuously curved axisymmetric models at zero angle of attack [1]. The latest version of this wall has variable porosity [3].

A cone-cylinder model is usually used to evaluate the wave-attenuating properties of the wall. These can be estimated by comparing the measured pressure distribution on the model with the theoretical one or with a pressure distribution obtained experimentally with a model that is so small in relation to the tunnel that the results can be considered as interference-free.

It could be stated, that the design criteria for the wall cross-flow characteristics and the methods to evaluate the wave-attenuating properties of the walls have resulted in test section wall configurations which are tailored to test axi-symmetric bodies at zero angle of attack. The tunnels are often, however, mainly used for development testing of airplanes and missiles. Some calibration tests with models of different sizes in relation to the test section have shown that although the wall interference is far from negligible, the results can in most cases be considered as acceptable for routine testing [4].

Little is however known about the requirements on the wall cross-flow characteristics for a lifting aircraft configuration. It is the objective of this investigation to study experimentally and theoretically the flow field around a lifting wing-body configuration at locations where wind tunnel walls are normally situated. The results might be used to establish relevant wall boundary conditions for this type of model.

If the cross-flow criteria resulting from this investigation agree reasonably well with the criteria used for the development of existing walls, the assumption that these walls are the most suitable also for routine testing will be confirmed. On the other hand, if the results disagree new ideas could be generated concerning necessary modifications of existing walls or possible new wall configurations.

After discussions with AFOSR Contracting Officer the research program has been split into two phases. During Phase 1, which this report covers, the preparations for the wind tunnel tests have been made. For the theoretical investigation the transonic computer program has been revised and the flow fields for some of the cases that will be tested have

been computed. During Phase 2 the wind tunnel tests will be performed and further theoretical computations will be made if the correlation between theory and experiment is reasonably good.

Mr. Hans Sörensén is responsible for the wind tunnel tests and Mr. Sven G. Hedman for the theoretical investigation. Mrs. Nada Agrell has assisted in carrying out part of the calculations.

2. EXPERIMENTAL INVESTIGATION

2.1 Test method and set-up

An experimental investigation has earlier been carried out in the FFA TVM-500 wind tunnel to determine the flow field in the vicinity of a wing-body configuration at M = 2.7 [5]. The experimentally determined near field formed the basis for a theoretical calculation of the far field. Hence the strength and position of the shock waves could be calculated at an arbitrary distance from a lifting body with complicated geometry.

The measurements were successfully made with good accuracy. It is therefore planned that this investigation is made with a new model at a low supersonic Mach number using the same test technique and to save costs using most of the test equipment.

Figures 1 and 2 show the test set-up. The model can be translated by a special support mechanism in the x-direction along the tunnel centerline during the test and it can also be rolled around the x-axis. The position of the flow inclination probe is fixed during a test run, but the radial position (y- and z-direction) can be changed between the runs.

2.2 Model, balance and sting

A new small model had to be manufactured. The size was chosen so that the waves generated by the model after reflection at the real wind tunnel wall do not interfere with the measurements at the hypothetical

wall (Figure 1). For measurements at $M_\infty = 1.2$ a model span of 70 mm has been chosen. The model is composed of an axisymmetric body and a delta wing typical for a supersonic fighter. The configuration chosen is geometrically similar to a larger model, which has earlier been extensively tested at FFA.

A two-view sketch of the general model arrangement is shown in Figure 3. and a photograph of the test set-up is shown in Figure 4. The model is manufactured by the FFA. The wing has a leading edge sweep back angle of 40°. The aspect ratio is 3.2 and the taper ratio 0.2. The wing profile parallel with the plane of symmetry of the body is a modified NACA-64A004 airfoil section. The construction of the model has required a thickened profile from $x/c = 0.5697$ to the trailing edge. The coordinates of the modified NACA-profile are given in Figure 5. The body is a circular cylinder with a pointed ogive nose section. The body and the wing are manufactured in one piece with an interchangeable nose-cone.

The model is mounted on a two-component strain gauge balance, Figure 6, and a sting. An exploded view of the model is shown in Figure 7.

2.3 Flow inclination probe

The hemispherical differential pressure yaw meter which will be employed for pressure measurements is shown in Figure 8. The pressure probe has a diameter of 3 mm. Four static-pressure orifices are located circumferentially 90° apart on the hemispherical surface and four on the cylindrical surface. A pitot-pressure orifice is located at the probe apex. The static-pressure orifice diameters are 0.5 mm and the pitot-pressure orifice diameter is 0.9 mm.

2.4 Tentative test program

The test program to be carried out during Phase 2 will include determination of local pressure coefficients and flow angle at a hypothetical test section wall. Measurements will be made along the centerline of the top, side and bottom walls for free stream Mach number, $M_\infty = 1.2$, and for two

"tunnel sizes". The model will be tested at 0°, 5° and 15° angle of attack.

3. CALCULATIONS BY MEANS OF A RELAXATION METHOD OF THE SUPERSONIC FLOW FIELD AROUND THE WING-BODY MODEL

3.1 Calculation procedure

3.11 Theory

The calculation method is described in [6].

A perturbation potential φ is defined in terms of the full velocity potential ϕ,

$$\phi(x,y,z) = U_{\infty} [x + \varepsilon \varphi(x,y,z)]$$

where the scaling factor ε is put $\varepsilon = \delta^{2/3} M_{\infty}$. δ is taken as the average wing thickness ratio. The transonic small disturbance equation is written in φ.

$$[(1-M_{\infty}^2) - (\gamma+1)M_{\infty}^2 \varepsilon \varphi_x] \varphi_{xx} + \varphi_{yy} + \varphi_{zz} = 0 .$$

This equation is put in finite difference form and solved by a relaxation procedure introduced by Murman and Cole [7]. The mixed flow character is obtained through the use of centered differences in subsonic portions and upstream differences in supersonic portions of the field.

The surface of the configuration may be written as $z = f(x,y)$. For field points adjacent to the body the boundary condition becomes

$$\varphi_z = \left(\frac{1}{\varepsilon} + \varphi_x \right) f_x + \varphi_y f_y$$

and for wing boundary points

$$\varphi_z = \frac{1}{\varepsilon} f_x .$$

The calculations of the flow field are made in points in a rectangular grid covering a finite domain of the physical space. The condition at the most upstream side of the box containing all the field points is $\varphi = 0$. No condition is forced on the most downstream side. At the remaining three exterior surfaces of the box the potential φ is put to zero. These surfaces are situated so far away from the model that effects from them should be negligible at the points investigated.

The pressure coefficient in the field is computed from

$$C_p = -2 \varepsilon \varphi_x \quad ,$$

and the flow angle from

$$\theta = \tan^{-1} [(\varphi_y + N \varphi_z)/(\frac{1}{\varepsilon} + \varphi_x)]$$

where $N = \pm 1$ for $y = 0$, $z \gtrless 0$.

In the absence of a shock fitting procedure shocks get smeared out over several mesh widths in finite difference calculations. In particular this is so when shocks are swept [8]. The calculations will not be able to give discontinuous changes in C_p and θ at the shock.

3.12 Application

The main portion of the calculations were performed in grid 1, described in the table below. To estimate the effect of the size of the box control runs were made in the slightly wider grid 2. The model positioned in grid 1 can be seen in Figure 9.

Grid	Type of calculation	No of points			Size in model scale		
		x	y	z	x	y	z
1	Main	37	40	27	-90/165	-294/294	0/286
2	Control	34	42	28	-63/142	-355/355	0/337

A relaxation factor of approximately one was used. The changes in the

flow field settled down at first in the upstream end and so during most iterations only the downstream portion was recalculated. 520 iterations were performed for the $\alpha = 0^{o}$ case. This solution was then used as a start for the 5^{o} incidence case and 340 more iterations were made. Small changes in the field were still observed in the planes $x = 142$ and $x = 165$.

The effects of the change of grid system were so small that they couldn't be seen in the plotted results.

3.2 Results

The model was a plane delta wing with a NACA 64A004 section mounted on an axisymmetric body, Figure 3.

Pressure coefficient, C_p, and flow deflection angle, θ, are presented at typical wind tunnel wall distances away from the model centerline, $y = 0$; $z = \pm 92, \pm 137$, and $y = 95, 149$; $z = 0$ respectively. Graphs of these functions appear in Figures 10a-11d. Please note that θ is defined positive for outflow from the model.

It is seen

- that the calculated pressure and flow angle vary continuously through the shocks, because of the used method of calculation and
- that effects due to lift decay faster than those due to thickness.

Figures 12 and 13 present the pressure coefficient as a function of the flow deflection angle for the wall positions investigated. These curves represent the required flow characteristics for an interference-free wall. It is obvious that it is not possible to find a fixed geometry configuration which is completely interference-free for this model.

Theoretical disturbance distributions for a cone-cylinder model with 2-percent blockage [1] at zero angle of attack are shown for comparison. In the outflow region the flow characteristics for the wing-body model are similar to those for the cone-cylinder, but in the inflow region

large differences occur. If these calculated results are confirmed by the experiments, this will be of importance, because the results indicate that the need of differential-resistance characteristics for the wall is much less pronounced in the expansion region of this three-dimensional lifting wing than in the expansion region of the cone-cylinder.

3.3 Conclusions and outlook

The small disturbance transonic flow program has been put to use for a supersonic flow condition and has given flow field characteristics to guide the calibration of a flow-inclination probe. Measured data will be available later for comparison. The part of the flow field influenced by the axisymmetric body only will later be calculated by a method containing a shock fitting procedure for better resolution at the nose bow shock.

REFERENCES

1. Goethert, B.H. — Physical aspects of three-dimensional wave reflections in transonic wind tunnels at Mach Number 1.20 (perforated, slotted, and combined slotted-perforated walls). AEDC-TR-55-45, March 1956.

2. Goethert, B.H. — Transonic Wind Tunnel Testing. Edited by W.C. Nelson. Published for and on behalf of AGARD by Pergamon Press, 1961.

3. Jacocks, J.L. — Comparison of variable porosity wall transsonic wind tunnel performance for upstream and downstream movement of the cutoff plates. ARO-AEDC-paper presented at the thirty-first Semiannual Meeting of the Supersonic Tunnel Association, April 24-25, 1969.

4. Binion, Jr., T.W. — An investigation of three-dimensional wall interference in a variable porosity transsonic wind tunnel. AEDC-TR-74-76, Oct. 1974.

5. Landahl, M. Sörensén, H. Hilding, L. — Research on the sonic boom problem. Part 2. - Flow field measurement in wind tunnel and calculation of second order F-function. NASA CR-2340, Nov. 1973.

6. Schmidt, W.
Hedman, S.G.
Recent explorations in relaxation methods for three-dimensional transonic potential flow.
ICAS Paper 76-22, 1976.

7. Murman, E.M.
Cole, J.D.
Calculation of plane steady transonic flows.
AIAA Journal, Vol. 9, No. 1, 1971.

8. Murman, E.M.
Analysis of embedded shock waves calculated by relaxation methods.
AIAA Journal, Vol. 12, No. 5, 1974.

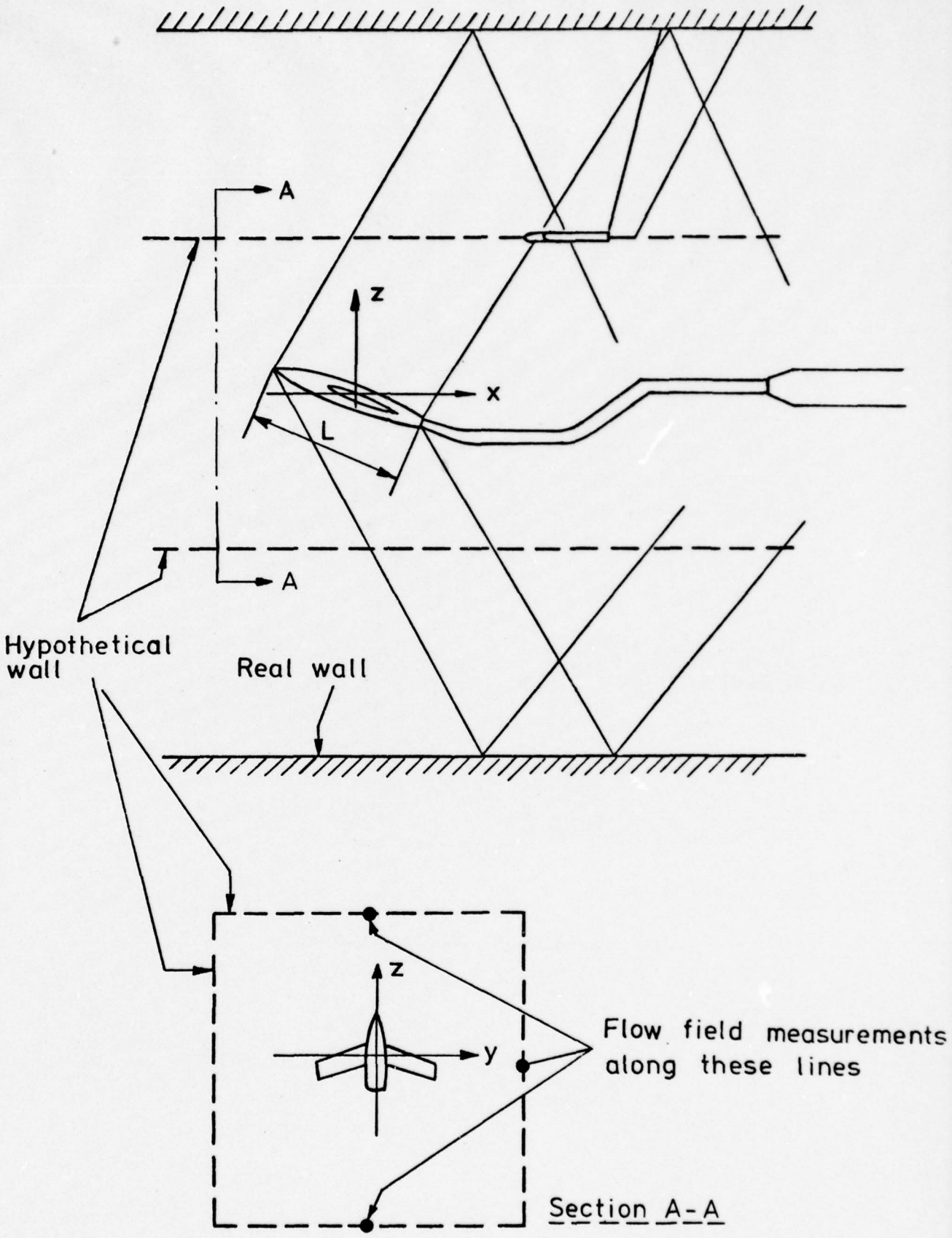

Fig. 1. Principle of test arrangement at M = 1.2.

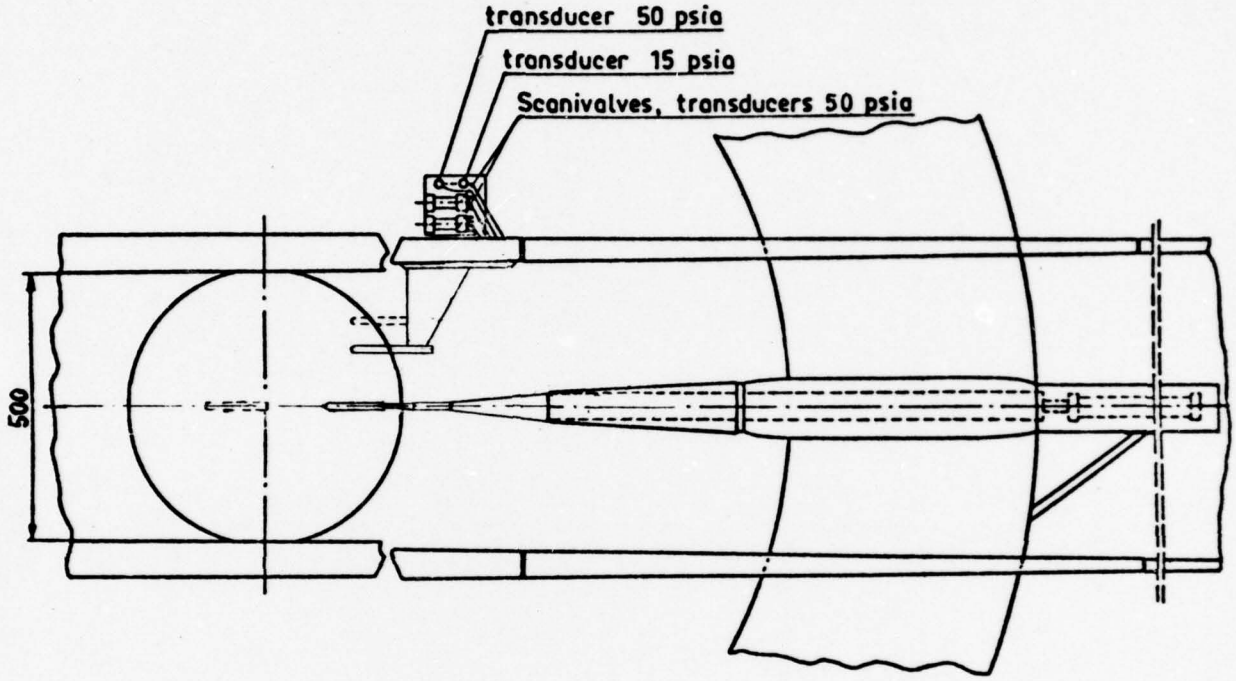

Fig 2. Schematical view of test set-up

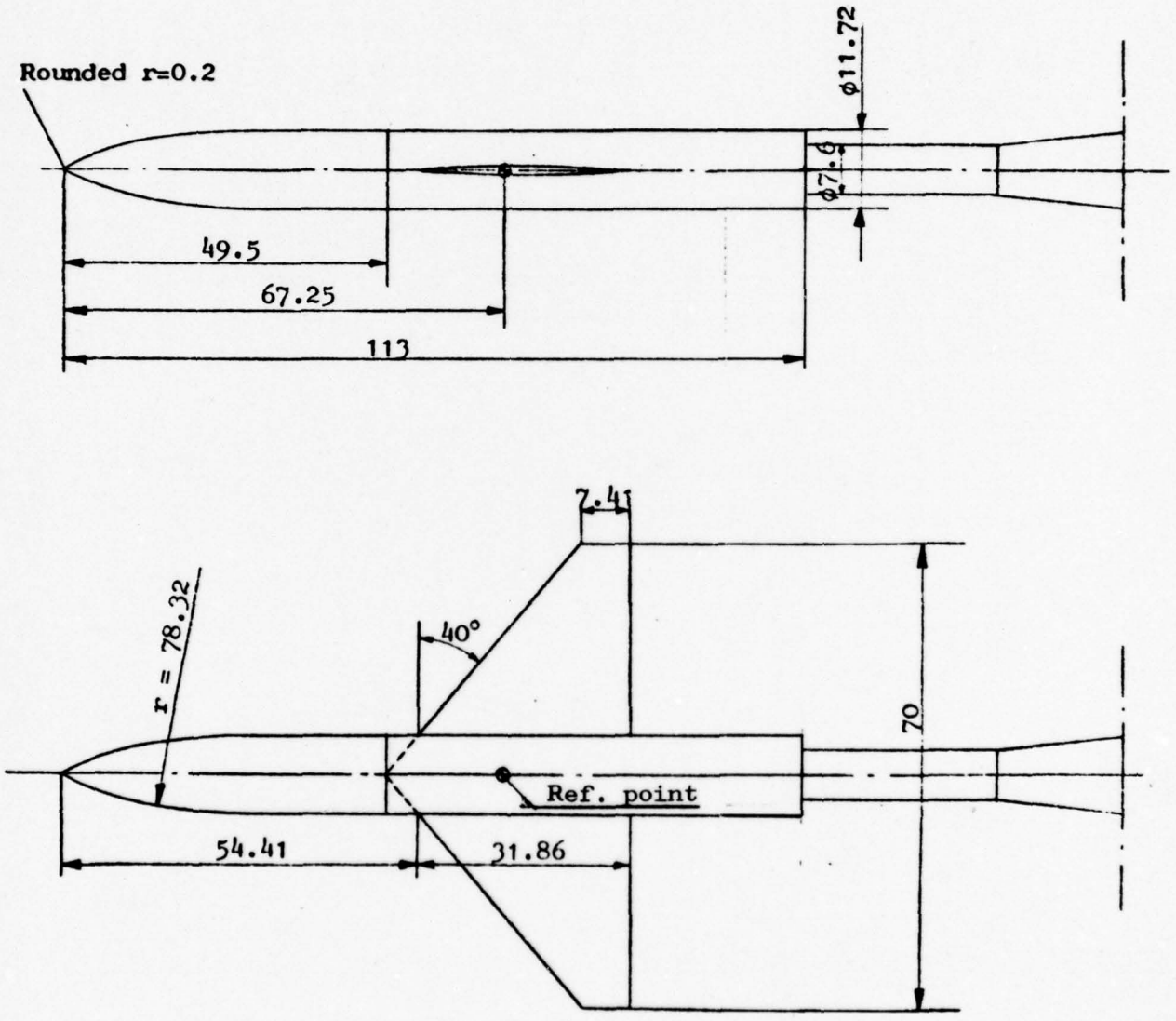

Fig 3. Wing body model design

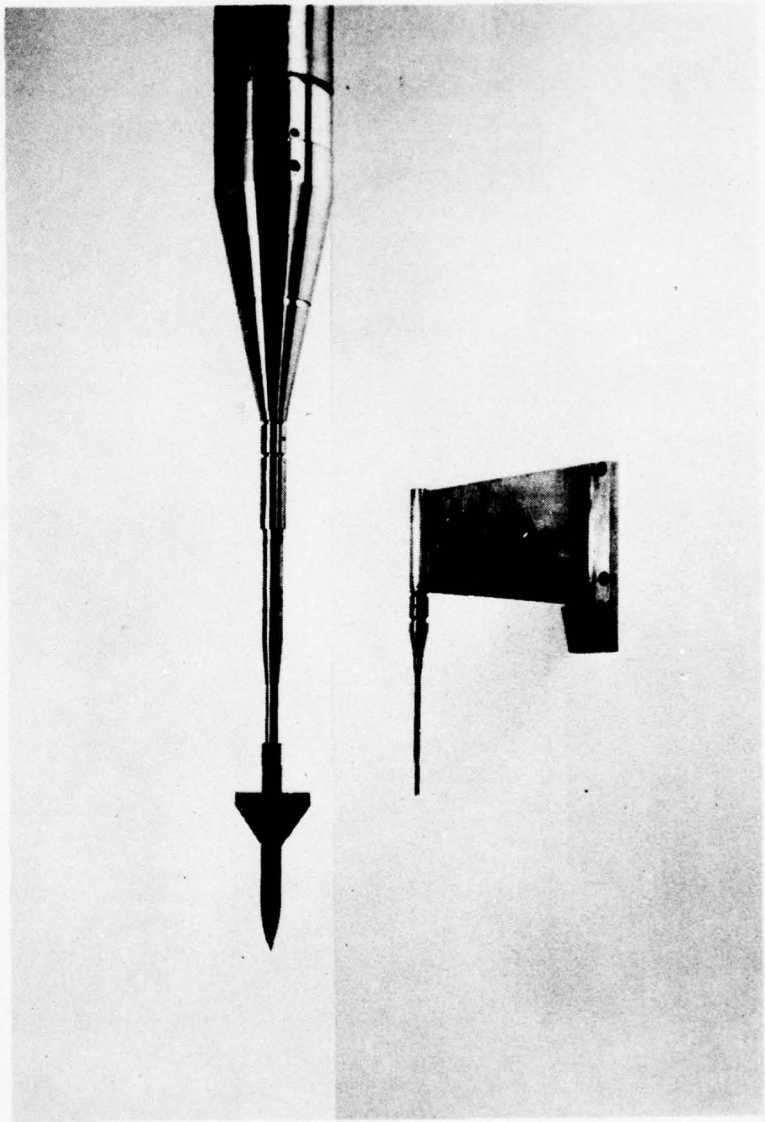

Fig. 4. Photograph of the test set-up.

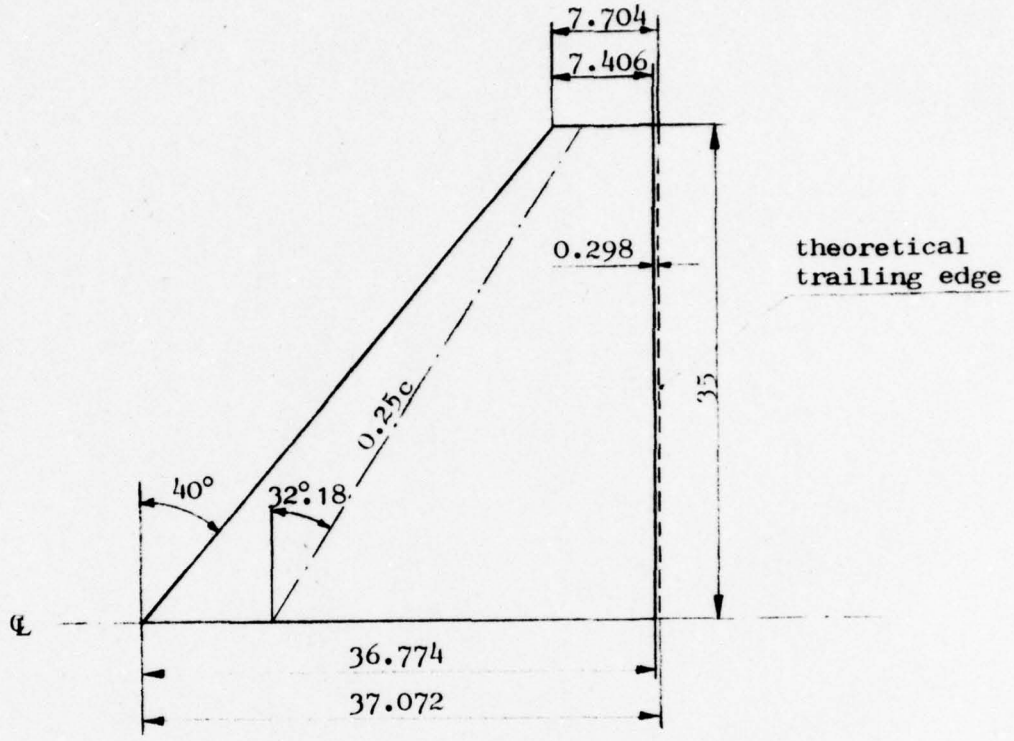

Aerofoil Section = Modified NACA 64A004

x/c %	z/c %	x/c %	z/c %	x/c %	z/c %
0	0	20	1.706	60	1.641
0.5	0.318	25	1.839	65	1.504
0.75	0.388	30	1.931	70	1.367
1.25	0.492	35	1.985	75	1.229
2.5	0.679	40	2.000	80	1.092
5	0.937	45	1.967	85	0.955
7.5	1.129	50	1.890	90	0.817
10	1.286	55	1.778	95	0.680
15	1.526	56.969	1.725	100	0.543

Fig 5. Wing data

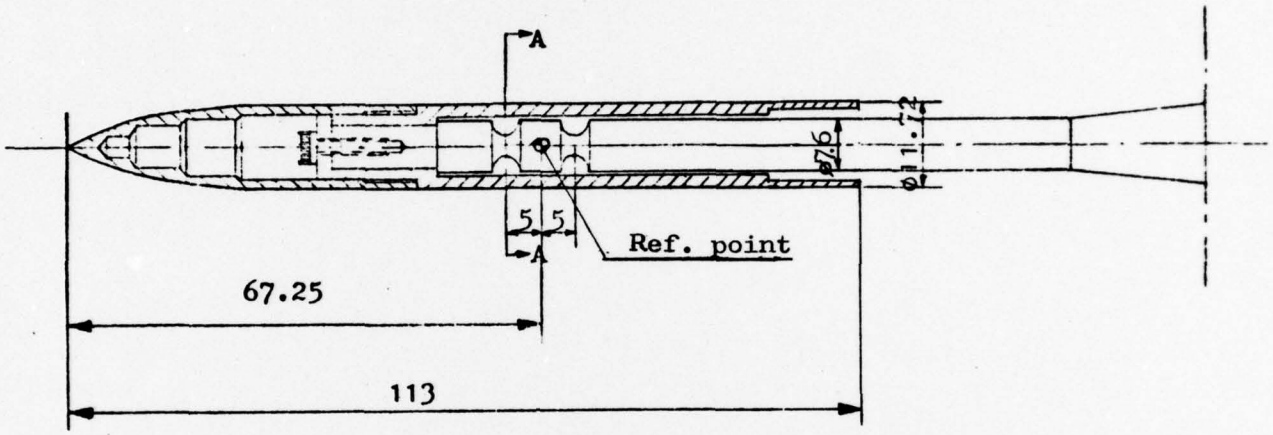

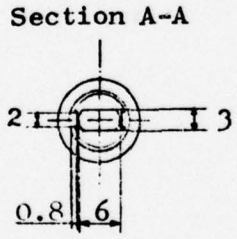

Fig 6. Two-component strain gauge balance

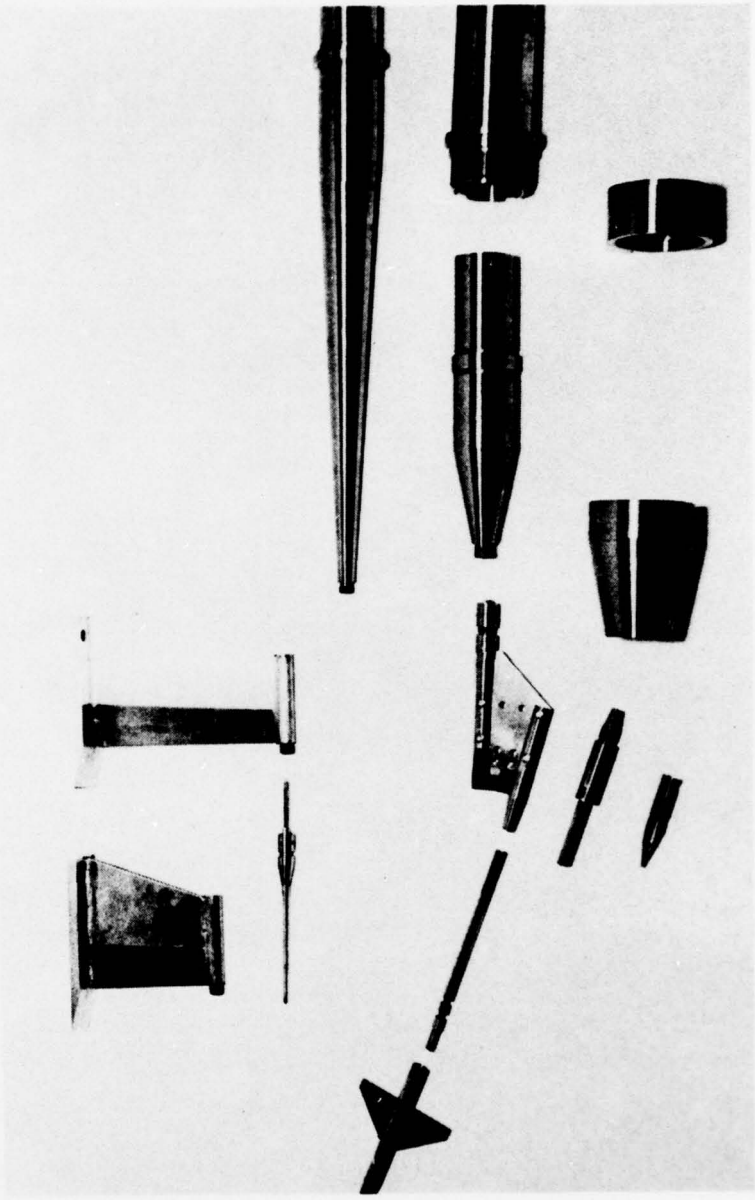

Fig. 7. Exploded view of the model.

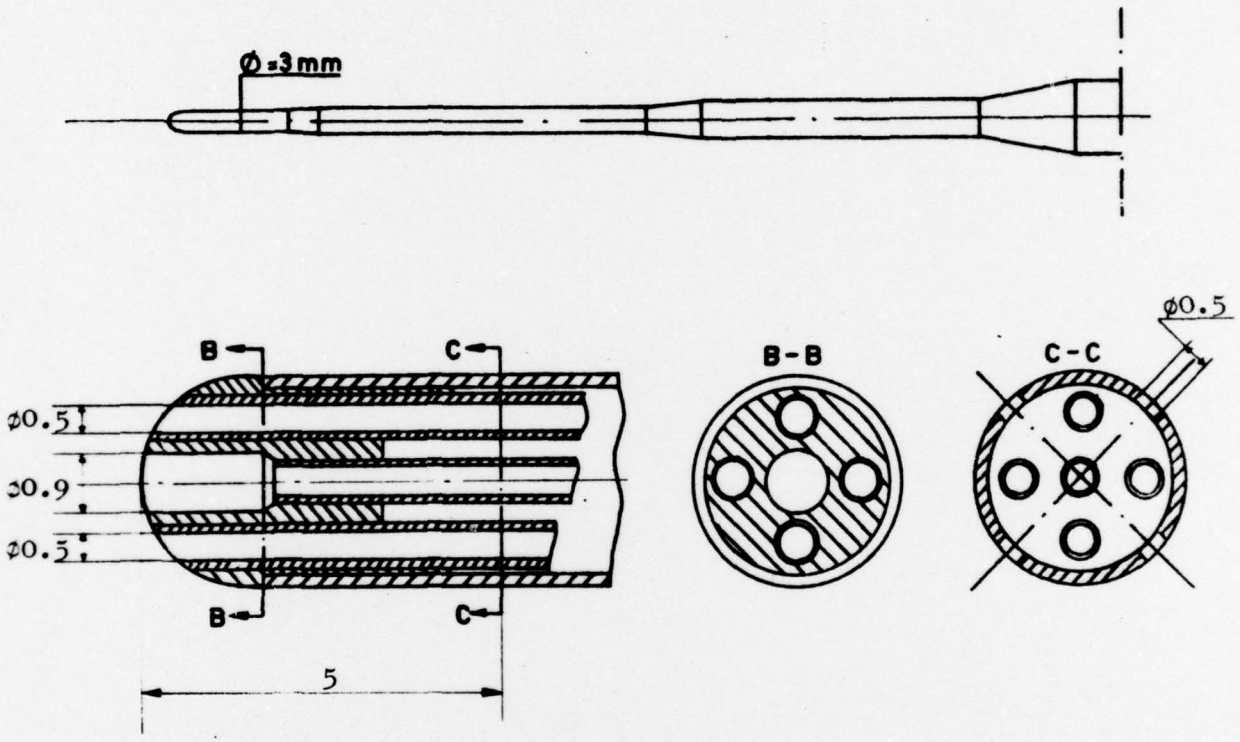

Fig 8. Design of yaw probe

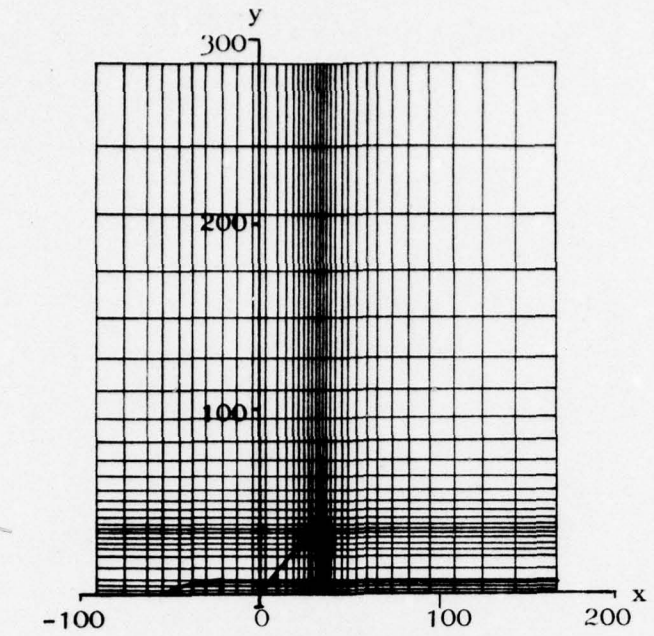

Top view

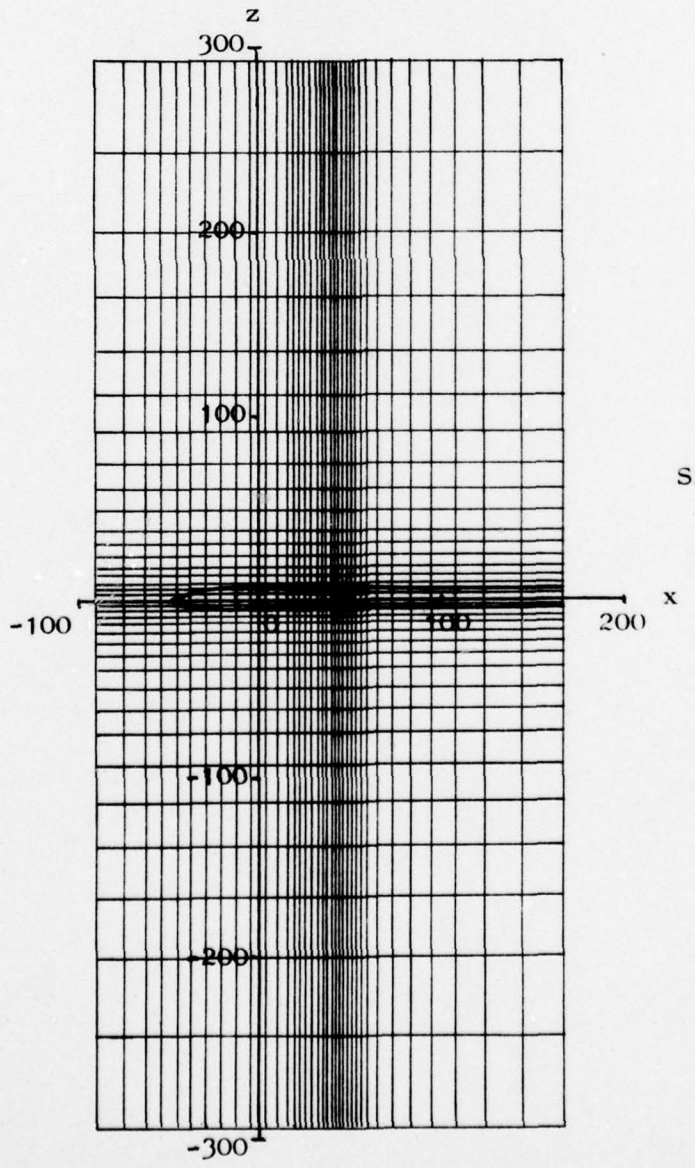

Side view

Fig. 9. Model in computation grid

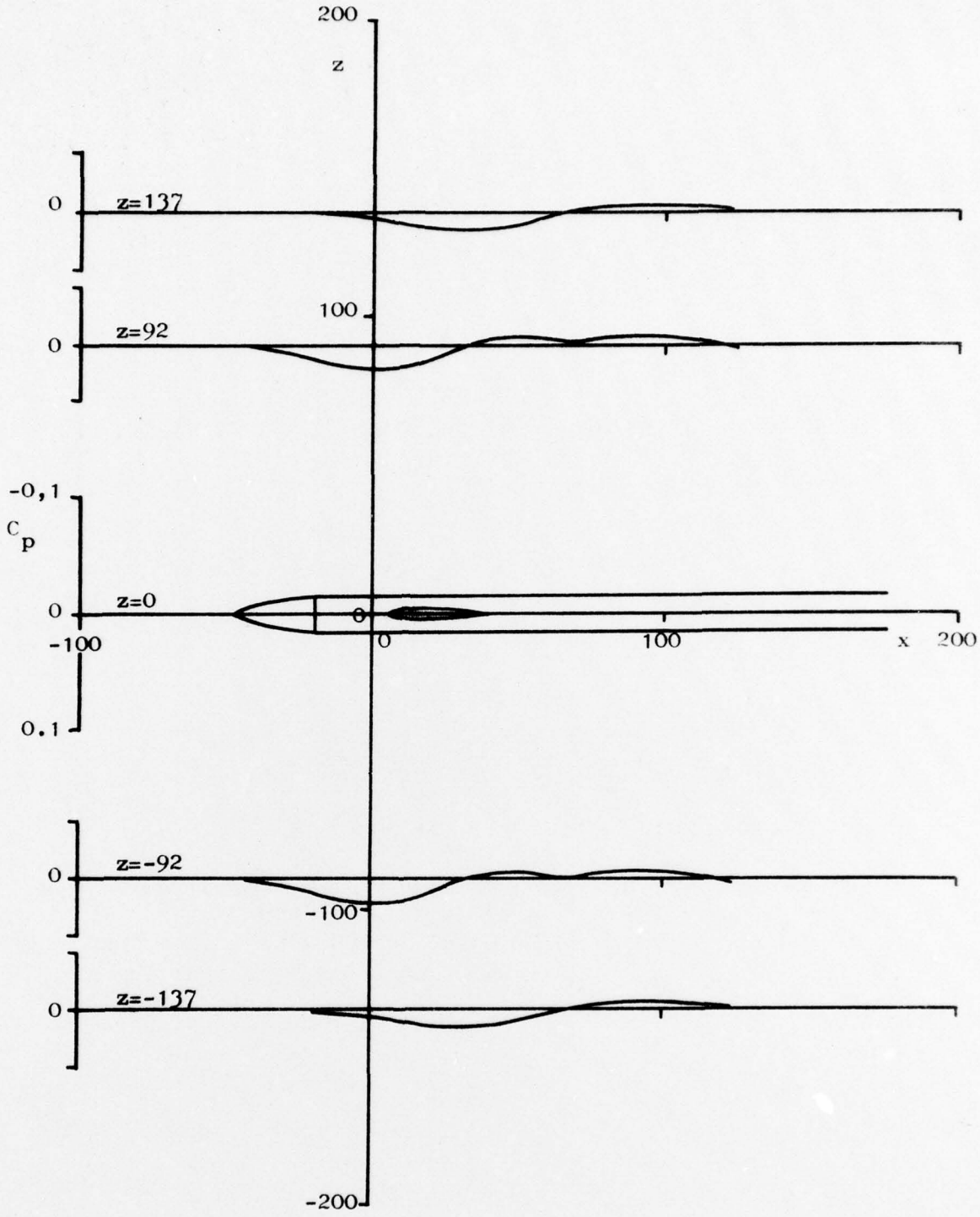

Fig. 10a. Flow field characteristics of wing-body configuration at $M_\infty=1.2$; $\alpha=0^\circ$
Pressure distributions at y=0; z=±92 and ±137

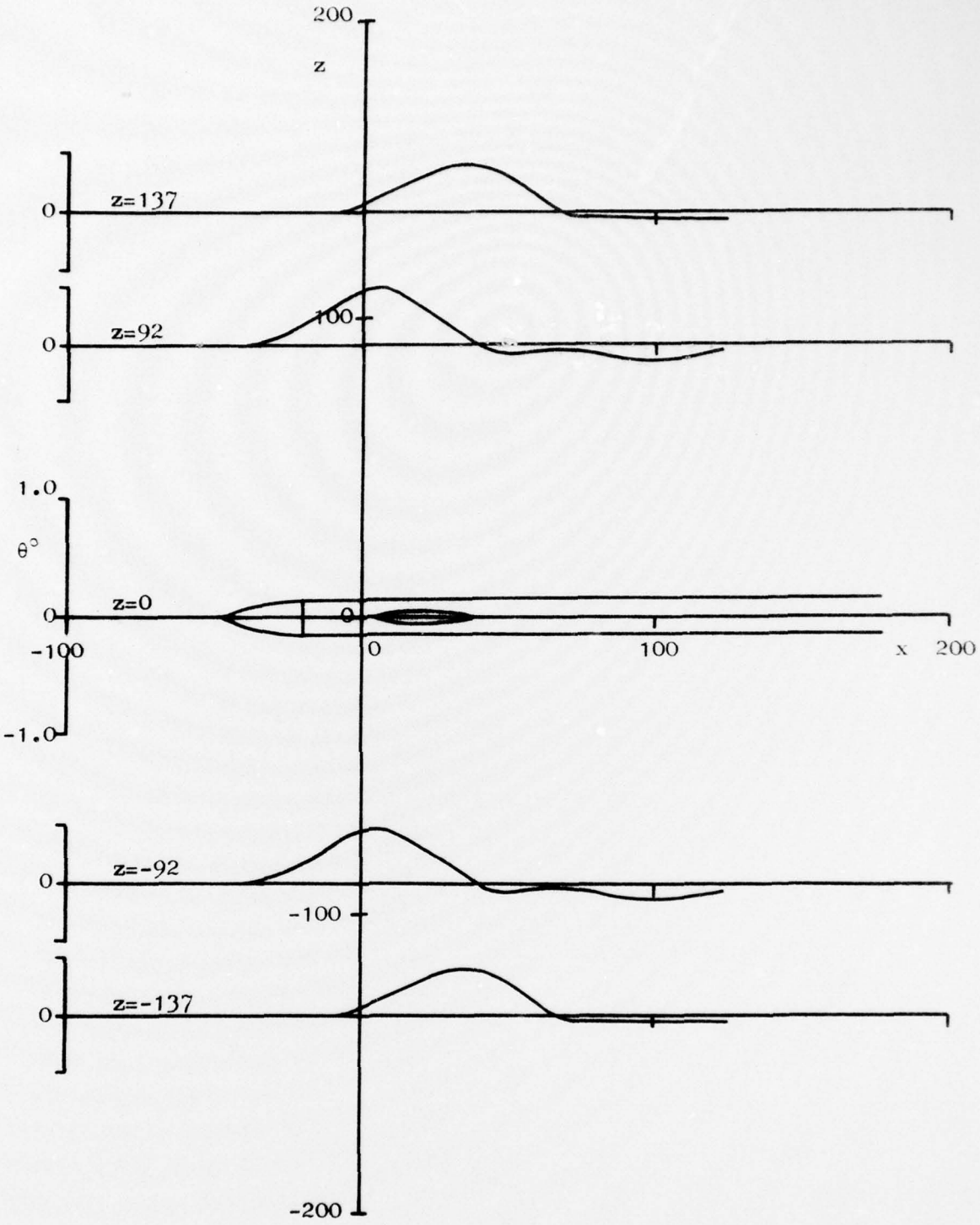

Fig. 10b. Flow field characteristics of wing-body configuration at M_∞=1.2; α=0°.

Flow angle distributions at $\dot{y}$=0; z=±92 and ±137.

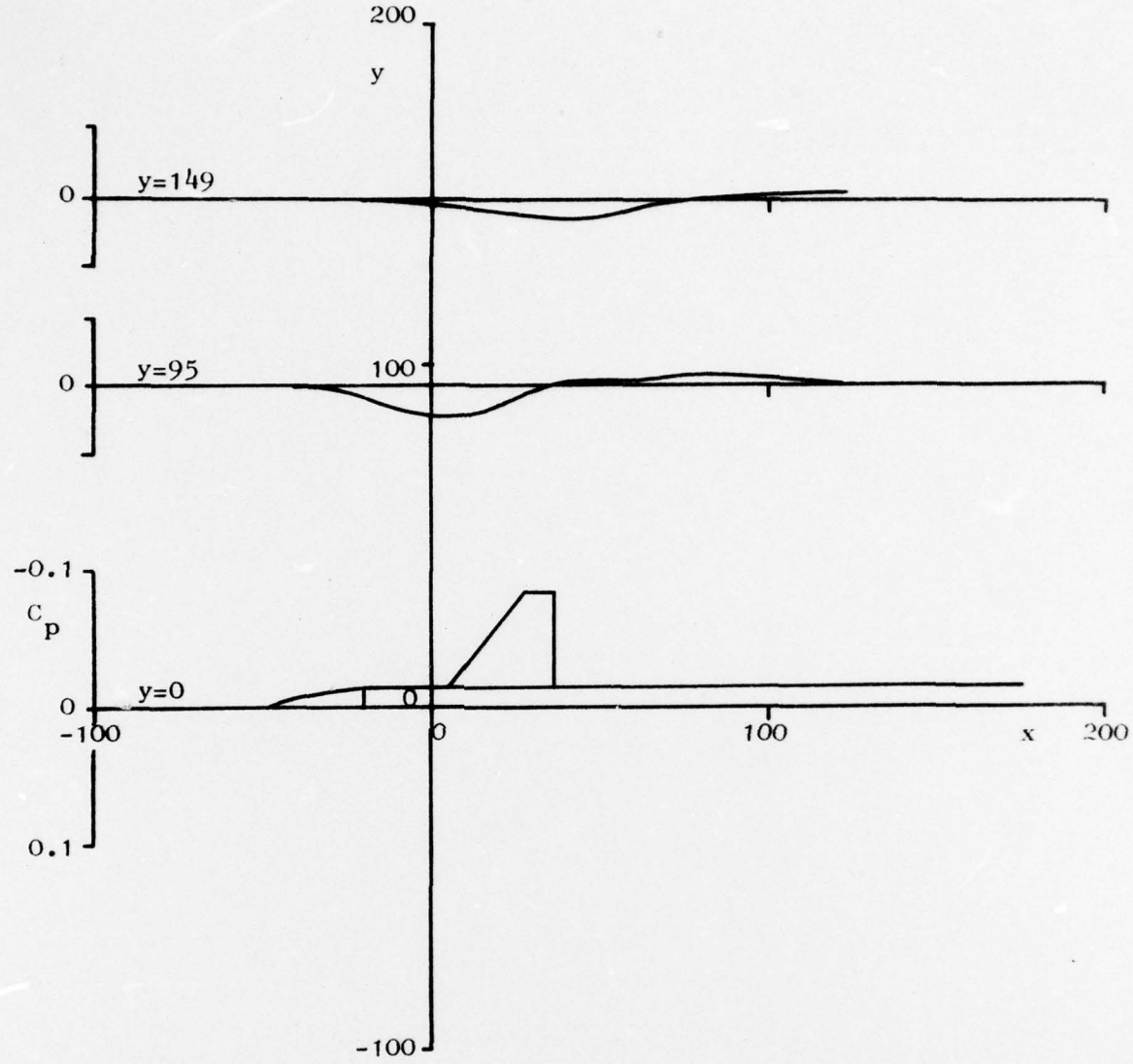

Fig 10c. Flow field characteristics of wing-body configuration at $M_\infty=1.2$; $\alpha=0^\circ$.

Pressure distributions at y=95 and 149; z=0.

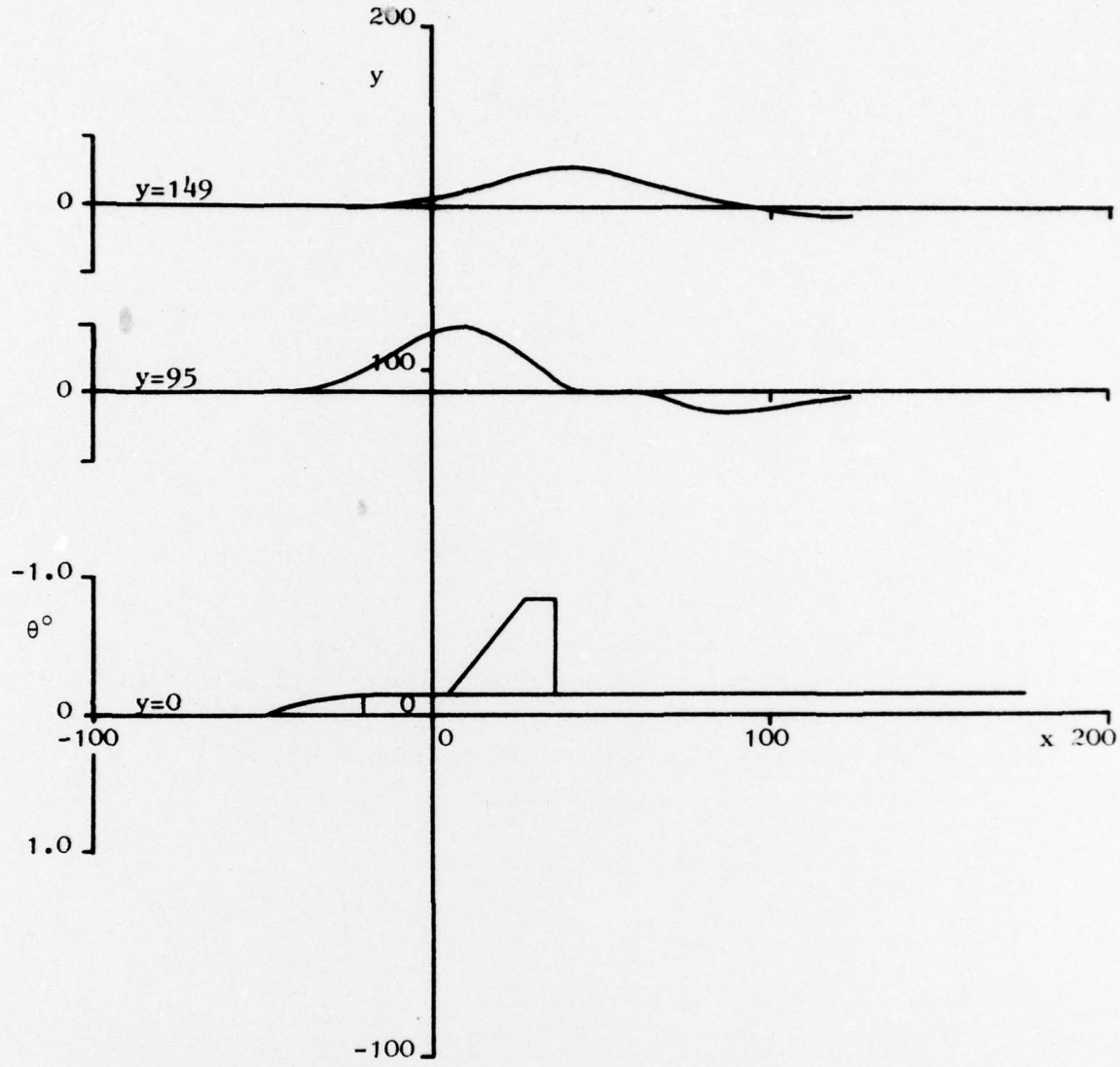

Fig 10d. Flow field characteristics of wing-body configuration at $M_\infty=1.2$; $\alpha=0^\circ$.

Flow angle distributions at y=95 and 149; z=0.

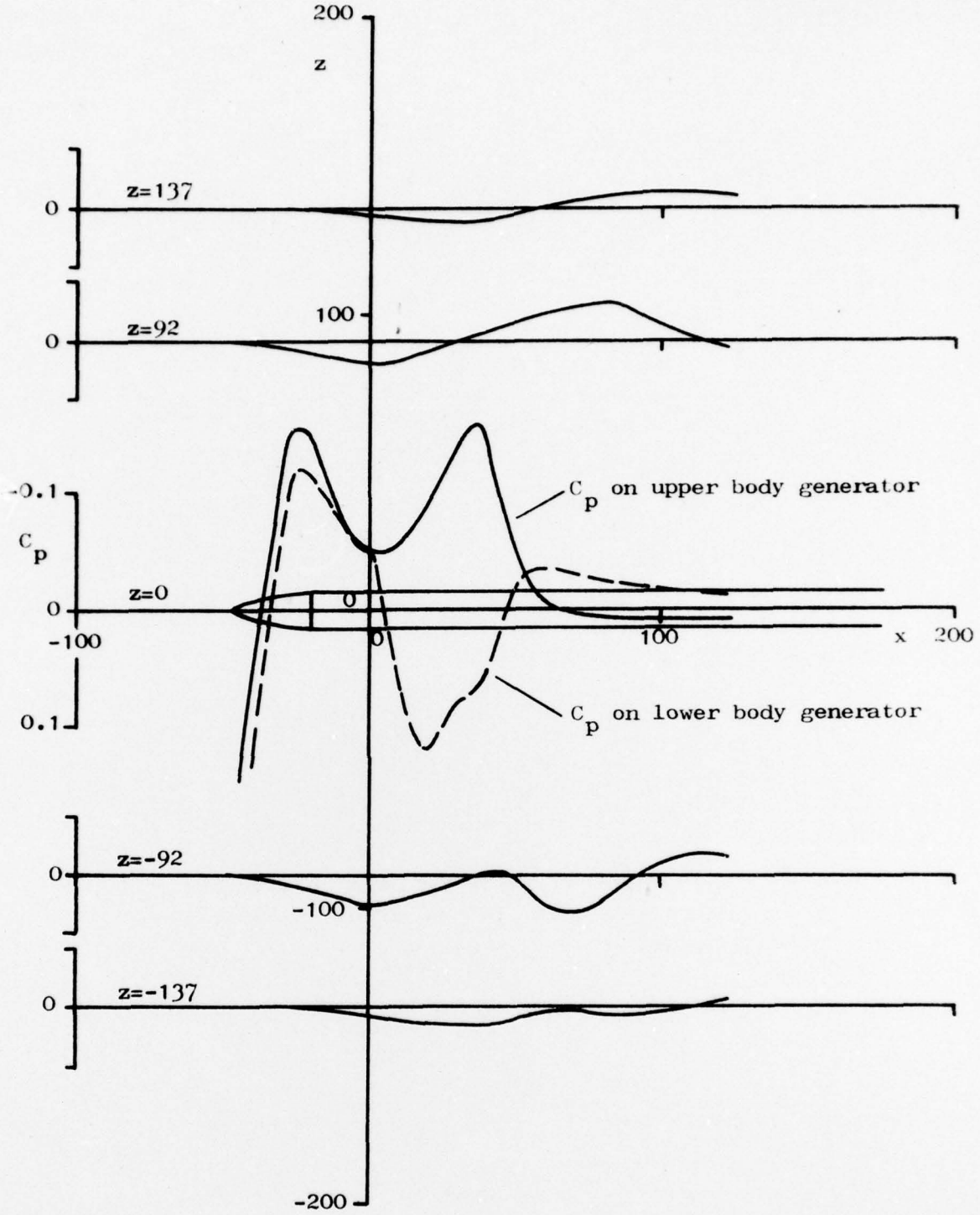

Fig. 11a. **Flow field characteristics of wing-body configuration at M_∞=1.2; α=5°.**

Pressure distributions at y=0; z=±92 and ±137.

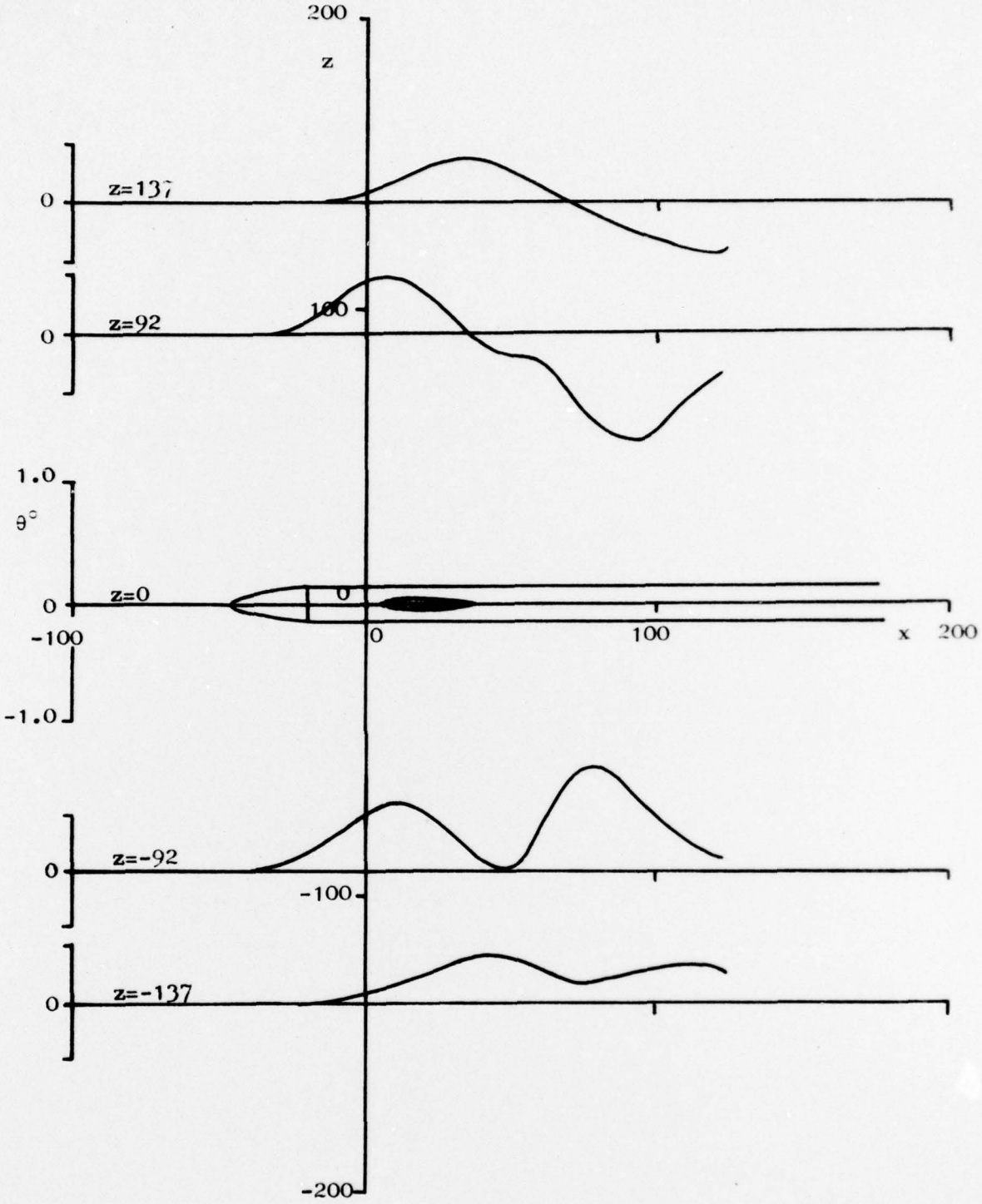

Fig. 11b. Flow field characteristics of wing-body configuration at $M_\infty=1.2$; $\alpha=5^\circ$.

Flow angle distributions at y=0; z=±92 and ±137.

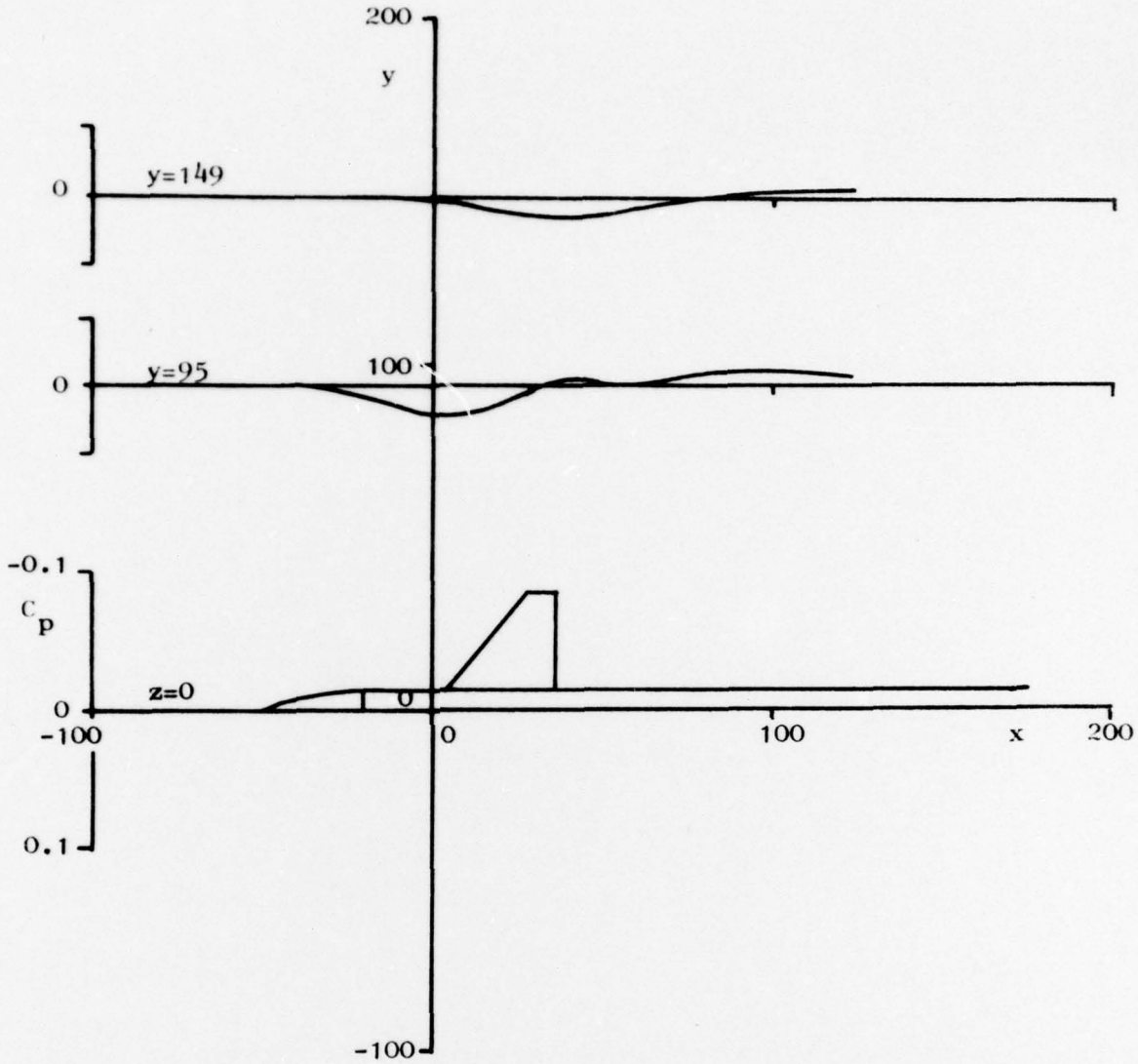

Fig. 11c. Flow field characteristics of wing-body configuration at $M_\infty=1.2$; $\alpha=5^\circ$.

Pressure distributions at y=95 and 149; z=0.

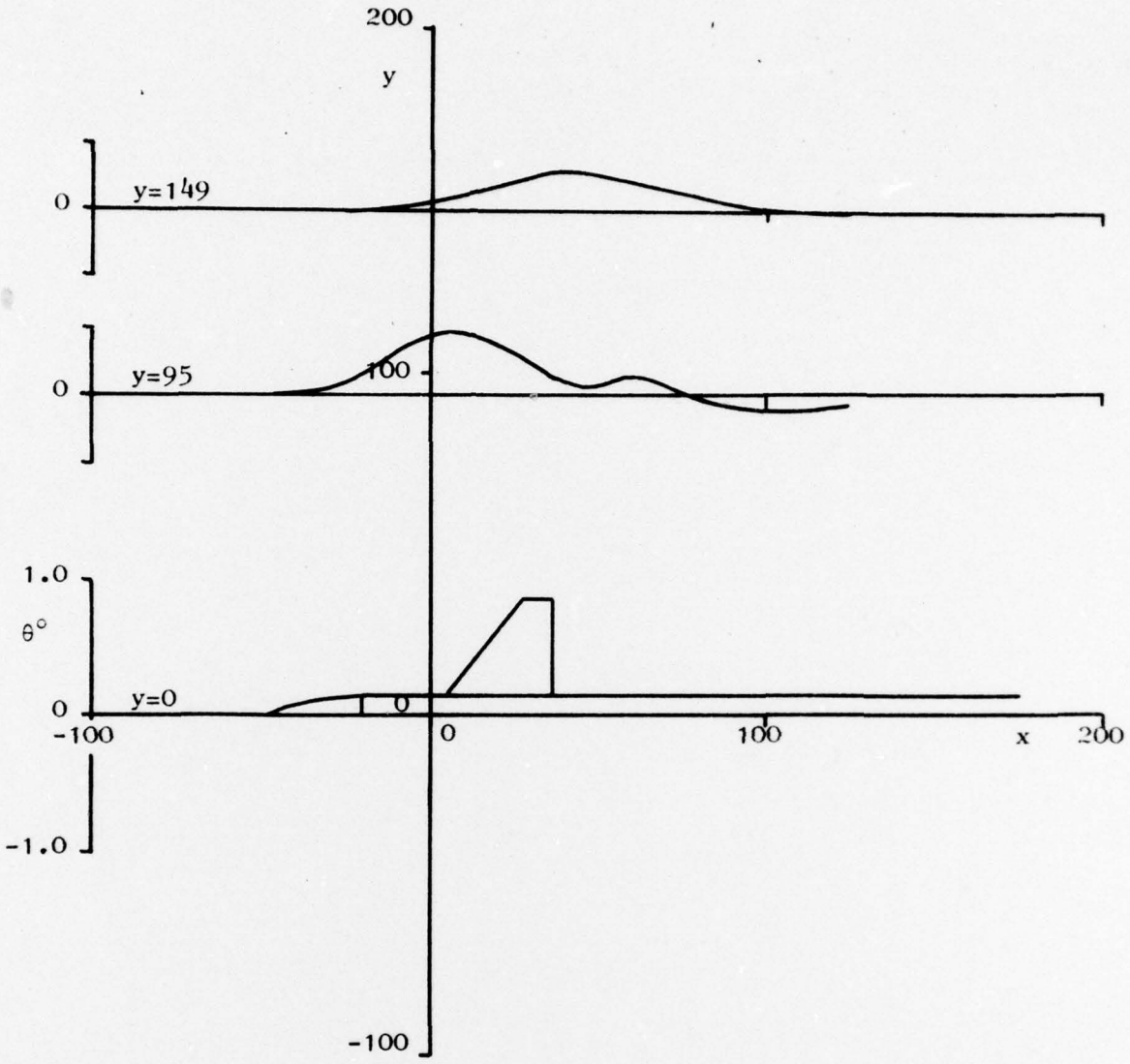

Fig. 11d. Flow field characteristics of wing-body configuration at M_∞=1.2; α=5°.

Flow angle distributions at y=95 and 149; z=0.

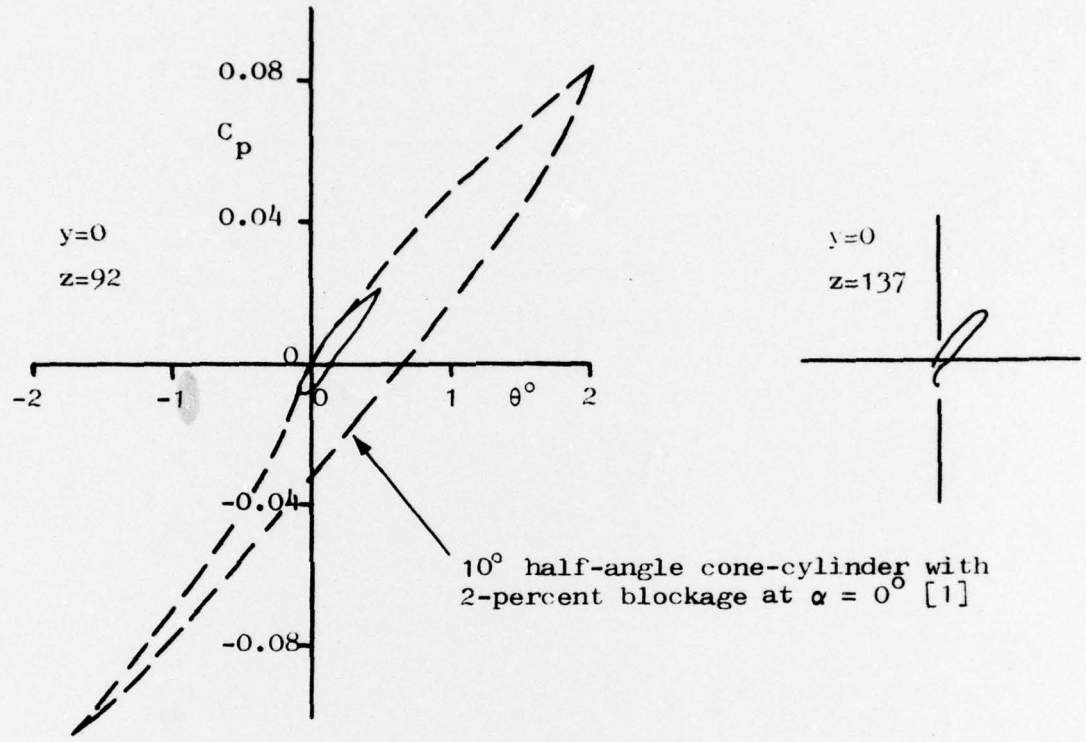

Fig. 12. Computed disturbance distribution due to wing-body configuration at M=1.2; α=0; y=0; z=92 and 137.

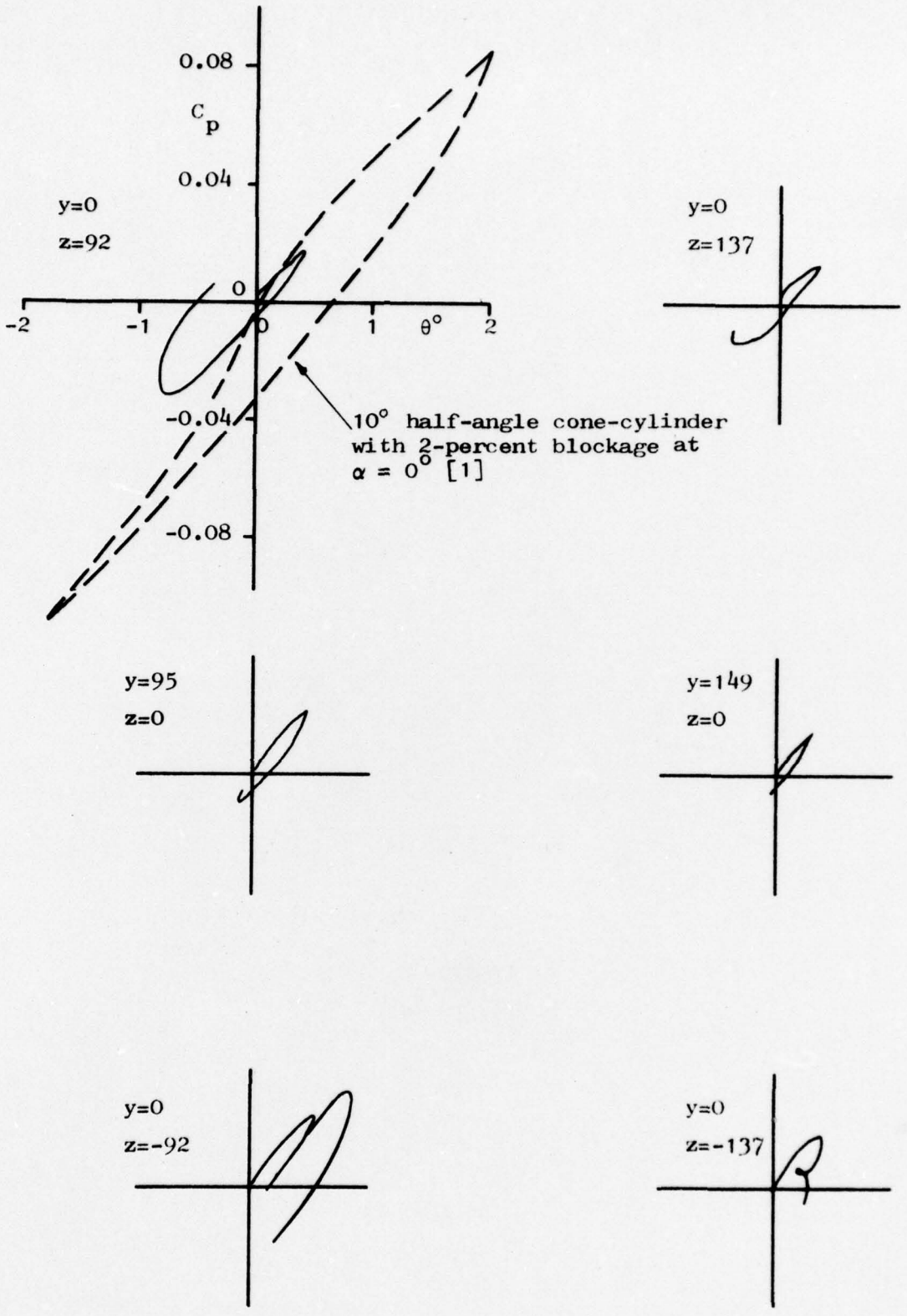

Fig. 13. Computed disturbance distribution due to wing-body configuration at M=1.2; α=5°.
y=0; z=±92 and ±137
y=95; z=0